ELSEVIER

International Journal of Adhesion & Adhesives 28 (2008) 340–349

International Journal of Adhesion & Adhesives

www.elsevier.com/locate/ijadhadh

Mode I fracturing properties of epoxy bonding paste

Elmar Karl Tschegg, Thomas Krassnitzer*

Laboratory for Material Sciences E138, Vienna University of Technology, Wiedner Hauptstraße 8-10, A-1040 Vienna, Austria

Accepted 13 August 2007
Available online 13 November 2007

Abstract

The wedge-splitting method by Tschegg was applied for the investigation of mode I fracture behavior of epoxy-based adhesives. Specific fracture energy and notch tensile strength of "traditional" thickened laminating resin were measured between −40 and +45 °C and compared to those of four new trial compounds. The adhesives in bulk were investigated as well as the interfaces between these adhesives and glass fiber-reinforced plastic. The wedge-splitting method has turned out suitable for epoxy resin. The quality of thickened laminating resin was not reached by the new trial compounds. Adherend pre-treatment with laminating resin and peel ply improved interfacial properties.

Keywords: Epoxy; Composites; Interfaces; Temperature influence

1. Introduction

1.1. Aim and scope

Composite components, such as those used in light airplanes, are subject to larger tolerances than metal parts, in particular due to variation in wall thickness. If such components are to be joined by bonding, gaps of several millimeters must often be bridged. The traditional adhesive for this application is "thickened resin", i.e., laminating resin with cotton fibers and, if necessary, thixotropic agent added. Similar adhesives are used in boat building and for wind turbine rotor blades.

Thickened laminating resin (TLR) has the advantage of high toughness combined with low mass density (approximately 800 kg/m^3), but it must be compounded manually, thus implying labor effort and variations in the mixture. The manual mixing is one of the reasons for the low mass density because it generates voids. There are aims to replace TLR by a "modern" bonding paste which can be mixed and dispensed by a machine. The present work compares the fracture mechanical properties of a "traditional" and four "modern" bonding pastes, which also consist of filled epoxy resin. It must be noted that the new bonding pastes were still at a developing stage at the time of the experiments.

Since adhesives are not normally subjected to direct stress, their tensile and compressive strength is only of subordinate interest. The properties of greater significance are shear strength and fracture mechanical properties. The latter can provide useful information on the damage growth behavior of an adhesive joint, which is a crucial aspect for composite airplanes. However, fracture mechanical values of bonding pastes *for light airplanes* are not publicly available.

The present work is, to the best of the authors' knowledge, the first published mode I fracture investigation of these materials. It is also the first investigation in which the wedge-splitting method was used for epoxy-based adhesives. The materials in bulk form as well as their interfaces to glass fiber-reinforced plastic (GFRP) were the subjects of the study.

1.2. Common test methods

A number of methods exist for the determination of the quality of an adhesive. The measurement of the pull strength between adhesive and adherend is the most simple

*Corresponding author. Tel.: +43 1 5880113724; fax: +43 1 5880113899.
E-mail address: e8726069@student.tuwien.ac.at (T. Krassnitzer).

0143-7496/$ - see front matter © 2007 Elsevier Ltd. All rights reserved.
doi:10.1016/j.ijadhadh.2007.08.006

method for interfaces. However, it reveals only one single value—the pull strength—which has only limited significance.

A more favorable approach is the determination of fracture mechanical values. The specific fracture energy G_F and the notch tensile strength σ_{ns}—both for the adhesive in bulk and for the interface between adhesive and adherend—provide useful information about the quality of an adhesive joint.

A common method to obtain bulk and interfacial mode I fracture mechanical values is the double cantilever beam (DCB) test. It requires consideration of the crack length to calculate the energy release rate, and it involves the risk of instable crack propagation. Testing of adhesives can also be accomplished with a DCB variant in which the two beams are forced apart by a wedge [1,2]. Other derivatives of the DCB method are the height-tapered cantilever beam (HTDCB) and the width-tapered cantilever beam (WTDCB) method. These eliminate the dependency on the crack length.

Mode I measurements can also be carried out using compact tension (CT) specimens [3], which are however more complex and therefore more expensive than wedge-splitting specimens.

Several methods are based on the loading of a notched specimen in tension, compression, or bending. Examples are the single-edge-notch bending (SENB) test [3] and the Brazilian disk (BD) specimen [4].

1.3. Survey of previous research

Mode I fracturing properties of epoxy resins *in bulk* have been studied extensively in the past, applying the methods mentioned above. The investigated adhesives include neat epoxy resin [5], blends with thermoplastic [6,7], and epoxy resins with various fillers, such as elastomeric particles [4,8–10], hollow or solid glass micro-spheres [11–13], glass fibers [13], spherical silica [14], carbon nano-fibers [15], or microencapsulated healing agent [16].

Mode I fracture mechanical properties of adhesively bonded *interfaces* were researched to a lesser extent. The particular combination of rubber-toughened epoxy resin and GFRP was studied by Kumar et al. [17].

2. Experiment

2.1. Principle of the test method

The wedge-splitting test [18,19] is used to determine the specific fracture energy G_F and the notch tensile strength σ_{ns} of brittle, quasi-brittle and ductile materials subjected to mode I cracking. The following is a brief description of the method. More details can be found in Ref. [19].

The wedge-splitting test is suitable for bulk materials as well as for interfaces between two materials (Fig. 1). The vertical force F_M is generated by a testing machine. It drives a steel wedge into the specimen's groove. The corresponding horizontal force F_H acts upon the vertical surfaces of the groove via steel rolls (or needle bearings) and two load transmission pieces, and thus acts to split the specimen. Friction is negligible because rolling friction is involved [19]. The crack opening displacement (COD) δ is measured in the line of the horizontal force.

A force vs. COD graph (e.g., Fig. 4) reveals the fracture behavior of the tested material: The notch tensile strength σ_{ns} (i.e., the ultimate tensile stress in the notch) is proportional to the maximum load, while the specific fracture energy G_F is the integral of the horizontal force with respect to displacement, divided by the cracked area. This demonstrates one advantage of the wedge-splitting method: the straightforward evaluation of the result which does not require consideration of the crack length. Further advantages are simple specimens in the shape of cubes, beams, or cylinders, and the possibility to use a simple loading device (which can even be a steel or aluminum frame with a manual spindle) [19].

In contrast to the usual, standardized methods, the wedge-splitting technique is designed to minimize the elastic energy stored in the test apparatus, specimen, and testing machine. When that elastic energy is less than the energy required to fracture the specimen, stable crack propagation will occur, and the force–displacement trace will continue beyond the peak force. The wedge-splitting test can thus deliver the specific fracture energy G_F of even brittle or quasi-brittle materials [20], e.g., concrete.

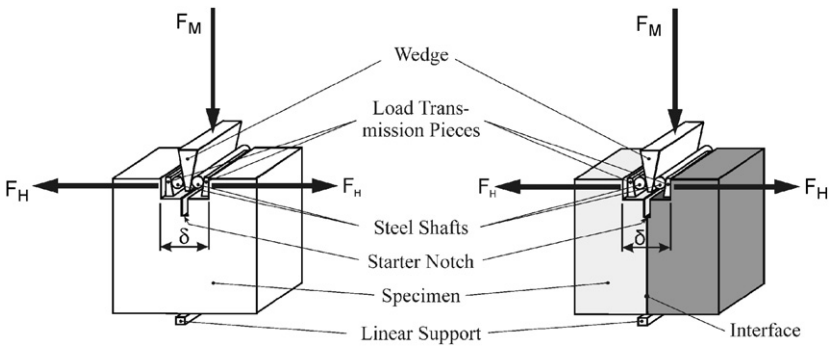

Fig. 1. Principle of wedge test by Tschegg.

Table 1
Weight percentages of fillers contained in bonding pastes

Bonding paste designation	Acronym	Hollow glass micro-spheres[a] (%)	Cotton fibers[b] (%)	Pyrogenic silicic acid (%)	Sil-Cell 300 (%)
Thickened laminating resin	TLR	–	9	–	6
Trial compound no. 1	TC 1	21	–	3	–
Trial compound no. 2	TC 2	18	4	1.5	–
Trial compound no. 3	TC 3	12	8	2.5	–
Trial compound no. 4	TC 4	15	4.5	2.5	–

[a]Diameter: 10% up to 20 μm, 50% up to 45 μm, 90% up to 75 μm, max. 85 μm.
[b]Cross section: reniform with dimensions (3–12) × (10–40) μm; length: approximately 0.4 mm.

2.2. Material specification

The adherend was in every case Isoval 11 rigid GFRP laminate, cut with a circular sawing machine. The "traditional" bonding paste, referred to as TLR, consisted of MGS L 285 bisphenol A-epichlorohydrin laminating resin and MGS 286 amine hardener, both supplied by Hexion Specialty Chemicals (Germany). This mixture was filled with cotton fibers and Sil-Cell 300 thixotropic agent, as shown in Table 1. Sil-Cell 300, made by Stauss-Perlite GmbH, Austria, is a micro-cellular filler, based on aluminum silicate, forming micro-bubble clusters (see SEM image, Fig. 10).

The new mixtures, referred to as trial compounds no. 1 through 4 (TC 1 through TC 4), were also made available by Hexion Specialty Chemicals. Rheological requirements place restrictions on the composition of bonding pastes. Accordingly, the amount and proportion of the fillers (see Table 1) were selected such as to make the mixtures suitable for mechanical dispensing and practical application. TC 1 through TC 4 furthermore contained pyrogenic silicic acid which acts as a thixotropic agent.

As described later, most of the comparative measurements were made with TLR and TC 1. Part of the measurements were subsequently repeated with TC 2, TC 3, and TC 4.

2.3. Specimens for wedge-splitting tests

Fig. 2 illustrates the specimens which were used for the investigation of the bonding paste in bulk and the bonding paste/GFRP interface. For both specimen types, two pieces were cut from Isoval 11 rigid GFRP laminate. After adherend pre-treatment (see next paragraph), the two GFRP pieces were positioned and aligned in a jig, leaving a gap of 10 mm which was filled with bonding paste. Curing took place at room temperature, post-curing was accomplished at up to 80 °C for approximately 24 h. The glass transition temperature of the investigated materials is always higher than the maximum curing temperature, i.e., above 80 °C in the present case. Finally, the starter notch was cut with a bandsaw, and a sharp nick was made on its ground with a razor blade.

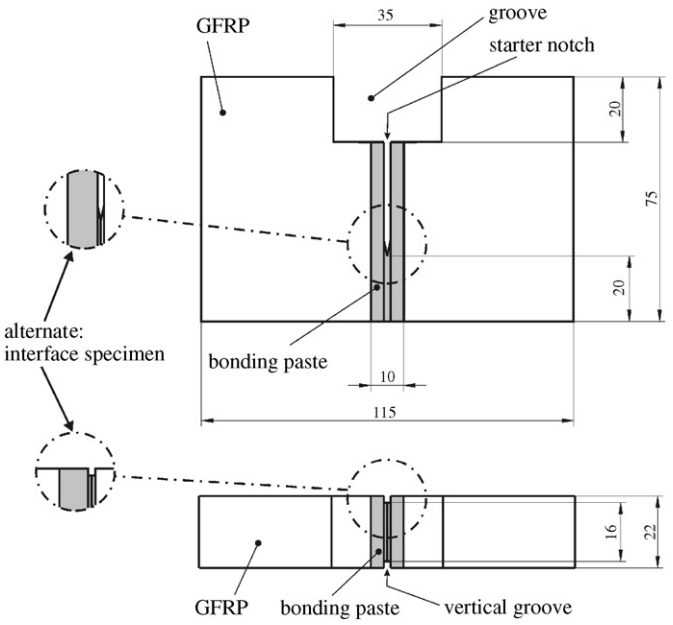

Fig. 2. Specimen for investigation of bonding paste. Main picture shows variant for test of bulk material, circular areas on left side explain variant for interface testing.

The glass layers within the GFRP pieces were aligned perpendicular to the interface. This is not the case in all engineering applications, but it is preferable for the wedge-splitting tests because it minimizes shear deformation of the GFRP pieces, and thus minimizes the elastic energy stored in the specimens. The results of the interfacial tests might be slightly affected by the orientation of the glass layers. The results for the adhesives in bulk are apparently not influenced by the glass layer alignment.

Different adherend pre-treatments were utilized, depending on the specimen type. In case of the bulk specimens, the bonding surfaces were coated with MGS L 285/286 laminating resin/hardener. The bonding paste was applied while the laminating resin was still wet. Since the crack ran through the bonding paste, the adherend pre-treatment had apparently no influence on the result. In case of the interface specimens, most of them were prepared with adherend pre-treatment, which consisted of peel ply that

was affixed with MGS L 285/286 laminating epoxy resin/hardener and peeled off after the resin had cured. This type of bonding surface is typical for light airplanes. In the present case, the resulting surface roughness corresponded to N11 (estimated with surface comparator). Some interface specimens with TC 1 were prepared without adherend pre-treatment for comparison.

2.4. Wedge-splitting test setup

Fig. 3 is a photograph of the specimen with the wedge device and the displacement gauges attached.

Loading of the specimens was done in a Schenck RSA 100 electrically driven tension–compression testing machine, with a crosshead speed of 2 mm/min.

The vertical force was measured with an electronic load cell with a capacity of 10,000 N and an accuracy of 0.1%. Since only the lowest 100 N of that capacity were used, a calibration check with standard weights was performed in this range. The displacement on both sides of the specimen (see Fig. 3) was measured with two linear displacement gauges. The signals from all three sensors were fed to a PC with measurement data card for the purpose of data display and recording at a rate of 20 Hz. The COD δ is the average of the "forward" and "rearward" displacement.

Measurements were carried out at room temperature as well as at low and high temperatures. The specimens were either heated to 50 °C in an electric furnace or cooled to −50 °C above liquid nitrogen. The specimen temperature was measured with a thermocouple which was inserted into a hole of approximately 20 mm depth in one of the two GFRP pieces. Since the test apparatus does not include heating or cooling, the hot or cold specimens were installed in it, and the actual test was started when the specimen had reached either +45 °C or −40 °C. During the test the temperature moved approximately 5 °C towards room temperature.

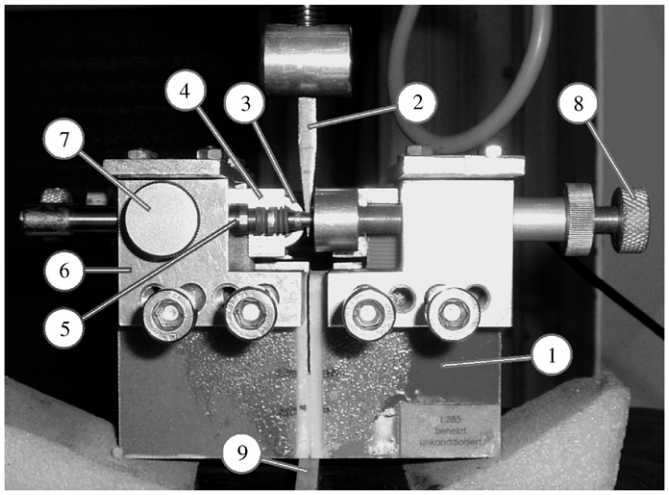

Fig. 3. Test setup: ① specimen, ② wedge, ③ needle bearings, ④ load transmission pieces (needle bearing mounts), ⑤ displacement gauge, ⑥ displacement gauge mount, ⑦ attachment screw for displacement gauge, ⑧ adjustment screw for displacement gauge, ⑨ linear support.

All in all, the test setup is simple enough to enable a test time of only a few minutes per specimen, which makes an environmental test chamber dispensable.

2.5. Pull strength tests

A few pull strength tests were carried out for comparison. Two bars with square cross section (22 mm × 22 mm) were cut from Isoval 11 rigid GFRP laminate. The glass layers within the laminate were oriented perpendicular to the interfaces. The two halves were adhesively connected by bonding paste. Analogous to the wedge-splitting specimens (see Section 2.3), "typical" bonding areas were created by pulling off peel ply, and specimens without this adherend pre-treatment were prepared for comparison. The tensile force from the testing machine was transmitted through spherical rod-end bearings screwed into both ends of the specimens. The crosshead speed was 1 mm/min. The tensile force was measured with an electronic load cell (capacity: 100 kN) and recorded at a rate of 20 Hz.

3. Results

Table 2 lists all specimens that were tested. Wedge-splitting specimens showing instable (sudden) crack propagation were rejected and are not included in the table. Where results of more than one specimen are available, the averages and coefficients of variation are furnished in the following.

3.1. Wedge-splitting tests for bonding paste in bulk

The first measurements were carried out at room temperature. TC 1 showed a higher notch tensile strength than TLR (see Figs. 4 and 5), but a significantly lower specific fracture energy, and is therefore expected to have unfavorable damage growth and fatigue properties. It must however be pointed out that the trial compound is not a commercial product yet. It was in fact a trial, and these were the first tests of its fracture mechanical properties.

The next step was the investigation of the influence of temperature on the fracture behavior. Both the notch tensile strength and the specific fracture energy of TLR decreased in case of hot and cold specimens, see Fig. 4. The F_H vs. δ plot at −40 °C suggests a higher notch tensile strength σ_{ns}. This is however the effect of differences in actual specimen geometry.

For trial compound no. 1, instable crack propagation was observed at low temperature, the corresponding specimens were thus rejected. The behavior at high temperature was similar to that at room temperature (Fig. 5).

Finally, three more trial compounds, referred to as TC 2, TC 3 and TC 4, were obtained and tested at room temperature. They were found to have a notch tensile strength similar to that of TC 1, but an improved specific fracture energy. This was achieved by reducing the content

Table 2
Specimen overview

Bonding paste designation	Acronym	Specimen temperature	Bulk specimens	Interface specimens	Pull strength specimens
Thickened laminating resin	TLR	Room temperature	3	4	2
		+45 °C	1	1	1
		−40 °C	1	–	1
Trial compound no. 1	TC 1	Room temperature	3	3+3[a]	2+2[a]
		+45 °C	1	1+1[a]	1+1[a]
		−40 °C	–	1+1[a]	1+1[a]
Trial compound no. 2	TC 2	Room temperature	3	–	–
Trial compound no. 3	TC 3	Room temperature	3	–	–
Trial compound no. 4	TC 4	Room temperature	3	–	–

[a]The same number of specimens were tested with and without adherend pre-treatment.

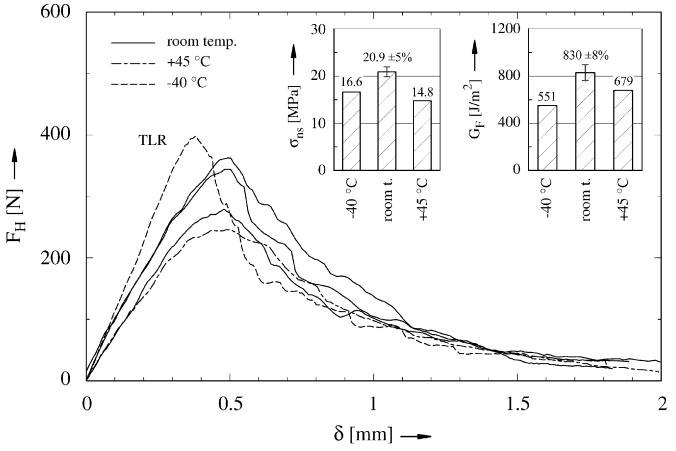

Fig. 4. Measurements on thickened laminating resin (TLR) in bulk form.

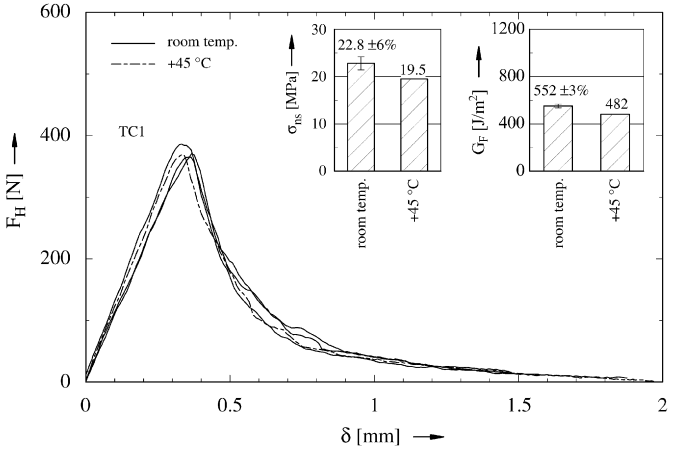

Fig. 5. Measurements on trial compound no. 1 (TC 1) in bulk form.

of hollow glass micro-spheres and adding cotton fibers to the resin (cf. Table 1). Three curves were recorded for each compound, which showed very little variation. Curves representing the average F_H vs. δ are shown in Fig. 6. Average curves for TLR and TC 1 at room temperature are included for comparison.

From the initial slope of the force vs. COD curve Young's modulus was approximated to be 2.3 GPa for TLR and 3.0 GPa for trial compound no. 1. This is a rough estimate using linear theory of elasticity and neglecting the multi-axial stress state in the specimen. The fundamentals of fracture mechanics are not yet developed to a level that allows the exact determination of Young's modulus from the available measurement data.

3.2. Wedge-splitting tests for bonding paste/GFRP interface

Each specimen was prepared such that the crack initiated at the interface. The crack path either remained entirely in the interface, diverted fully into the bonding paste, or diverted partially (i.e., over part of the specimen's width) into the bonding paste. Since the crack path has a strong impact on the load vs. displacement curve, it is depicted as part of the test result for each specimen.

For the evaluation of G_F only those specimens were considered which had a purely interfacial crack, and for σ_{ns} only those specimens were considered in which the crack was either fully or partially interfacial. All other measured values were omitted because they showed arbitrary variations due to the partial or full deviation of the crack into the bulk material.

In case of the TLR (see Fig. 7) tested at room temperature, the crack never remained entirely within the interface. In two specimens it diverted partly into the resin, and in two specimens it diverted fully into the resin. The crack in the specimen tested at +45 °C also diverted fully into the resin.

In case of trial compound no. 1 with adherend pre-treatment (see Fig. 8) tested at room temperature, two specimens had a purely interfacial crack and one had a crack that fully diverted into the bonding paste. The crack in the specimen tested at +45 °C also diverted fully into the bonding paste. The crack in the specimen tested at −40 °C remained within the interface.

In case of trial compound no. 1 without adherend pre-treatment (see Fig. 9) tested at room temperature and

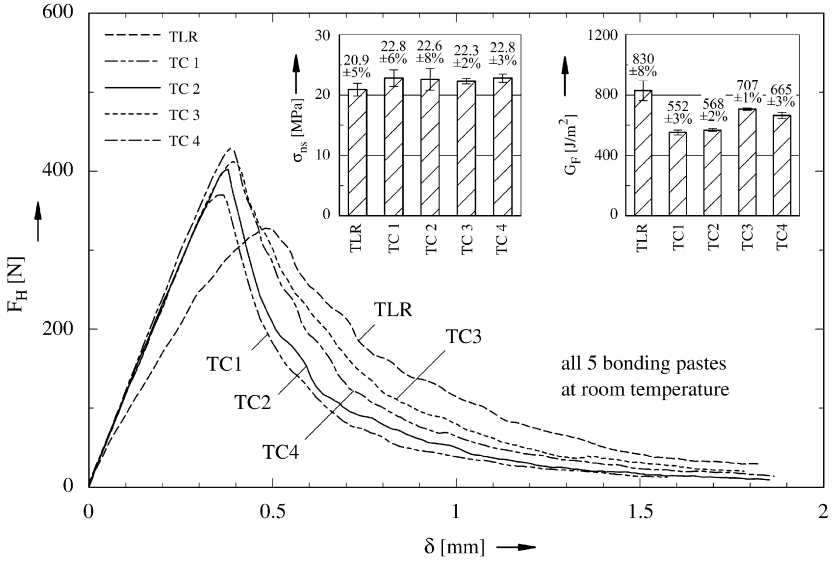

Fig. 6. Comparison of all five bonding pastes, in bulk form, averaged over three specimens each.

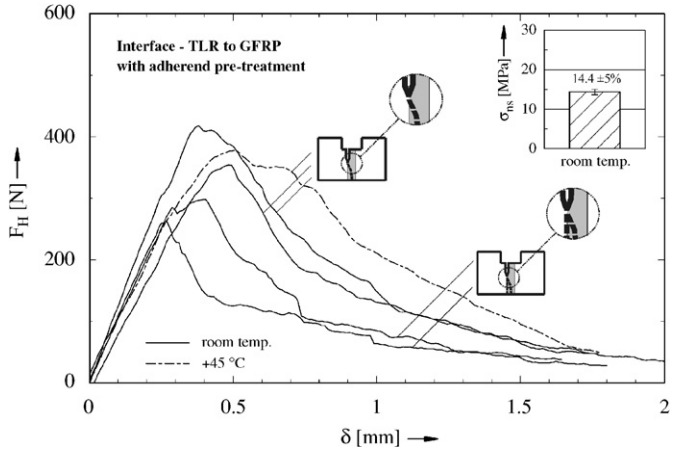

Fig. 7. Interfacial crack of thickened laminating resin (TLR)/glass fiber-reinforced plastic (GFRP).

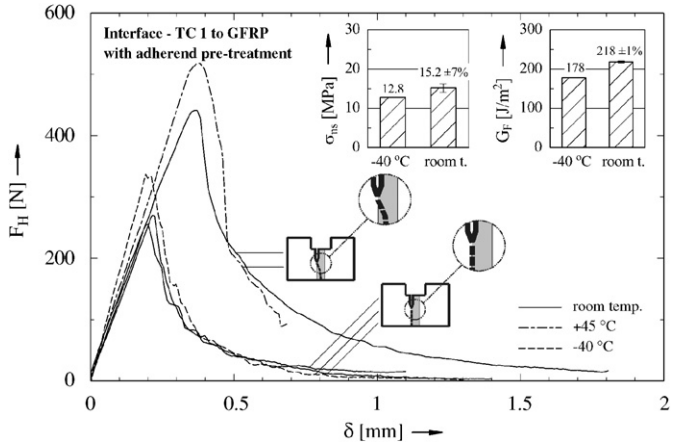

Fig. 8. Interfacial crack of trial compound no. 1 (TC 1)/glass fiber-reinforced plastic (GFRP) with adherend pre-treatment.

+45 °C, the cracks were fully interfacial. The crack in the specimen tested at −40 °C partly diverted into the bulk material.

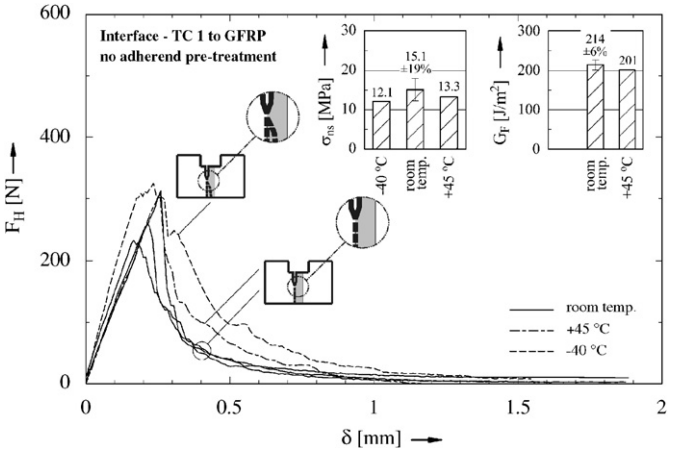

Fig. 9. Interfacial crack of trial compound no. 1 (TC 1)/glass fiber-reinforced plastic (GFRP) without adherend pre-treatment.

3.3. SEM images of bonding paste/GFRP interface specimens

Figs. 10 and 11 are SEM images showing the area where the crack deviated from the interface into the bonding paste.

In case of TLR (Fig. 10), the interface is located in the left hand area of the image. The constituents of the adherend, i.e., glass fibers and matrix, can be identified. Note that the glass layers are oriented perpendicular to the plane of the image. In the right hand half, showing the cracked bonding paste, one can identify the cotton fibers and two types of nearly spherical cells embedded in the resin. The first type are Sil-Cell micro-bubble clusters that have a cross linking similar to wood cells [21]. Such cross-linked areas increase the fracture toughness of the adherend due to the energy absorbed during crack progression. The second type are voids filled with air. The thin layer of pure laminating resin between GFRP and

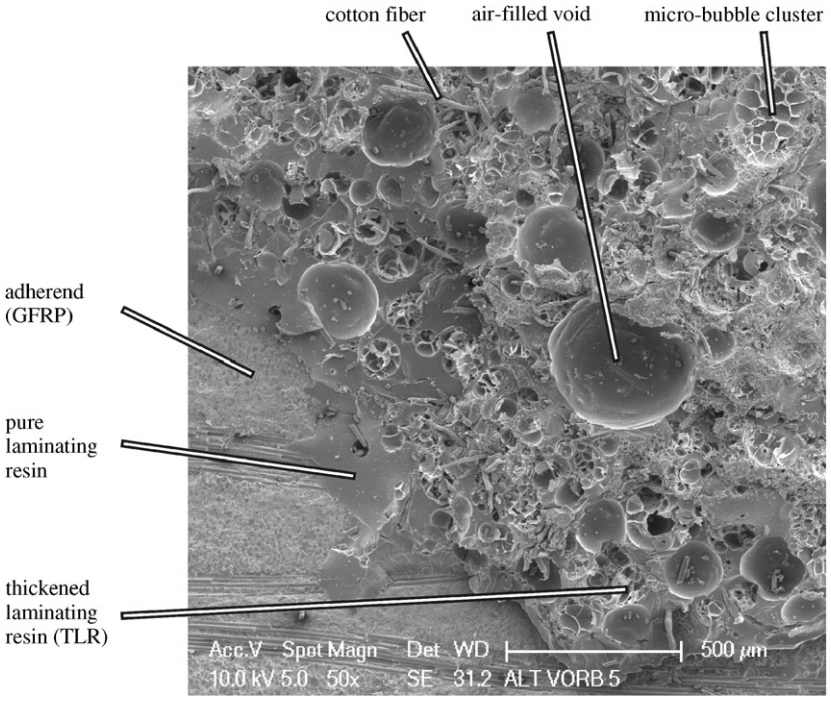

Fig. 10. Thickened laminating resin (TLR), tested at room temperature; transition between interfacial crack and cohesive crack.

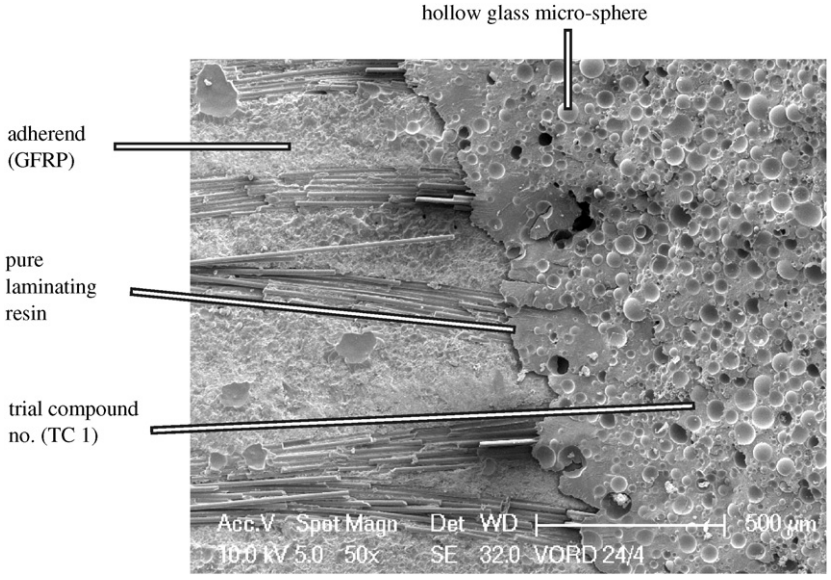

Fig. 11. Trial compound no. 1 (TC 1) with adherend pre-treatment, tested at +45 °C; transition between interfacial crack and cohesive crack.

bonding paste, which constitutes the adherend pre-treatment, is visible at the borderline between adherend and adhesive.

The image showing trial compound no. 1 with adherend pre-treatment (Fig. 11) shows the adherend in the left half. Similar to Fig. 10, the constituents of the adherend can be identified. Some small (approximately 100 µm) pieces of resin have remained on the interface. The cracked adhesive is seen in the right half of the image. The circular spots show the spaces occupied by the hollow glass micro-spheres. The individual glass micro-spheres have either fully remained in the resin, were completely torn out of the resin (i.e., have remained on the other half of the specimen), or were cracked.

3.4. Pull strength tests for bonding paste/GFRP interface

The results of the pull strength tests are shown in Fig. 12. TLR and TC 1 both have their highest pull strength at low temperature. TC 1 is appreciably stronger than TLR under equal conditions. Its pull strength declines slightly when the adherend is not pre-treated.

4. Discussion

4.1. Suitability of the test method

The wedge-splitting method is apparently suitable for epoxy-based resin. The large majority of the measurements delivered curves which are stable (i.e., no rapid drop in force) and reproducible. Comparing the results to those obtained in previous research (see Table 3), one can see that they are of a plausible magnitude. Where parameters were varied in the other author's studies (e.g., filler percentage or particle size), only the highest values are listed.

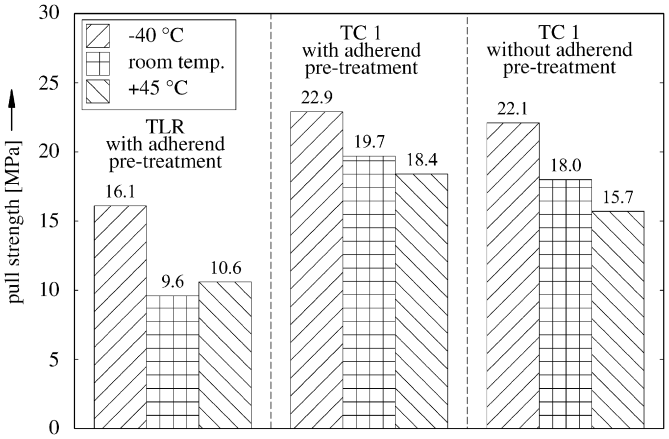

Fig. 12. Results of pull strength tests on thickened laminating resin (TLR) and trial compound no. 1 (TC 1).

4.2. Comparison of the different materials

Generally, TLR has a smaller σ_{ns} but a higher G_F than all new bonding paste blends (TC 1–TC 4). This result can be attributed to the higher content of cotton fibers which, during crack progression, absorb more energy than the hollow glass micro-spheres. TLR is therefore superior in terms of crack resistance.

In case of the interfaces, TLR and trial compound no. 1 have approximately the same notch tensile strength. The specific fracture energy could not be compared because a purely interfacial crack never occurred in TLR. This material's increased tendency of crack deviation is an advantage because the specific fracture energy increases as the crack runs into the bulk adhesive (cf. Fig. 7).

The pull strength of trial compound no. 1 is approximately twice as high as that of TLR (see Fig. 12). Omitting the pre-treatment of the adherend results in approximately 10% decrease in pull strength. As discussed earlier, the pull strength is not a very relevant value.

4.3. Comparison of G_F for bulk material and interfacial crack

The available results for G_F allow a comparison between trial compound no. 1 in bulk and the corresponding

Table 3
Comparison with results of previous research

Reference	Type of test[a]	Material	Method[b]	K_{IC} (MPa m$^{1/2}$)	E (GPa)	v [1]	G_{IC} (J/m^2)
This study	B	TLR	WS	~1.5[c]	~2.3	–	830[d]
This study	B	TC 1	WS	~1.4[c]	~3.0	–	552[d]
[4]	B	Epoxy resin with elastomeric particles	BD	1.68[e]	3.52	0.36	800[e]
[6]	B	Epoxy resin blended with PEK-C thermoplastic	SENB	1.24	2.29	–	560[f]
[10]	B	Epoxy resin with rubber particles	CT	4.42	~3.25[e]	–	~6000[c]
[11]	B	Epoxy resin with hollow glass micro-spheres	SENB	~3.1[c]	~3.5[e]	–	~2800[e,f]
[12]	B	Epoxy resin with solid glass micro-spheres	SENB	2.31	4.87	0.366	1096[c]
[14]	B	Epoxy adhesives filled with spherical silica	SENB	~1.7[e]	4.05	0.36	~620[c]
[15]	B	Epoxy resin with carbon nano-fibers	SENB	2.35	~3.1	–	~1550[c]
[16]	B	Epoxy resin with "healing fluid" embedded in microcapsules	HTDCB	1.25	2.8	–	560[c]
This study	IF	TC 1 on GFRP adherend	WS	–	–	–	218[d]
[17]	IF	Epoxy adhesive with rubber particles on GFRP adherend	DCB	–	–	–	1254

[a]B, bulk resin; IF, resin/GFRP interface.
[b]WS, wedge splitting; BD, Brazilian disk; SENB, single-edge-notch bending; CT, compact tension; HTDCB, height-tapered double cantilever beam; DCB, double cantilever beam.
[c]Calculated using either $G_{IC} = K_{IC}^2/E$ (plane stress condition) or $G_{IC} = K_{IC}^2(1-v^2)/E$ (plane strain condition), depending on the assumption of the corresponding authors.
[d]Value at room temperature; G_F equals G_{IC} for brittle materials.
[e]Read from chart.
[f]The highest G_{IC} was measured for neat resin, i.e., without additives.

interface specimens without adherend pre-treatment. Both at room temperature and at +45 °C, the interfacial G_F is approximately 40% of the bulk G_F.

4.4. Effect of surface roughness

The effect of surface roughness can be seen from a comparison of the results of trial compound no. 1 with and without adherend pre-treatment (Figs. 8 and 9). G_F and σ_{ns} values are slightly higher for the interfaces with pre-treatment. The improvement is smaller than the statistical uncertainty due to the low number of specimens, nevertheless it agrees with theory according to which a rough surface generally increases the interfacial strength. In cases where the crack remains in the interface, the greater effective area of a rough surface and/or the energy required to tear small pieces out of the adherend or the adhesive increase the fracture toughness. If the surface roughness causes the crack to deviate into the adhesive, then this deviation increases the fracture toughness as well, as was proven by measurement (see Fig. 8 for example). There may be combinations of adhesive and adherend however for which a crack deviation into the adhesive or adherend leads to a decrease in fracture toughness.

4.5. Comparison between wedge-splitting test and pull strength test

The pull strength test which is most often used for interface testing yields only one isolated value with limited significance, and no fracture mechanical values. The wedge-splitting test reveals far more information, namely the specific fracture energy required to break the joint, and an estimate of Young's modulus which can be derived from the initial slope of the force vs. COD graph. Fig. 6 illustrates the difference between a more brittle (e.g., TC 1) and a more ductile material (e.g., TLR). TC 1 has a higher notch tensile strength, but TLR's specific fracture energy is significantly higher.

In the present study, the results of the pull strength test (see Section 3.4) may suggest that the new bonding paste is superior to TLR. The wedge-splitting tests (see Section 3.2) have shown however that this is not the case. Again it must be noted that the new bonding paste was still under development and therefore the desired properties were not yet reached.

4.6. Size effect

Wedge-splitting tests carried out in the past on concrete specimens revealed a "size effect". In the present study, the size of the plastic zone was estimated using fracture-mechanical methods. These calculations have shown that the size of the plastic zone in the bulk bonding paste is an order of magnitude smaller than the width of the adhesive gap (10 mm, see Fig. 2). In case of interfacial cracks, the plastic zone is even smaller. The size effect may therefore be expected to be negligible.

4.7. Outlook

There is a need for further research to investigate the effect of specimen conditioning including ultraviolet radiation, as well as an extension of the temperature range. Moreover, the mode II crack behavior should be examined, because this is the failure mode of a "properly" loaded bonded joint.

5. Conclusions

1. The wedge-splitting method by Tschegg [18,19] has turned out suitable for the investigation of epoxy-based adhesives. Reproducible measurements of fracture mechanical values were made both for adhesive in bulk and for the interface between adhesive and GFRP. The required specimens and test facilities are simple.
2. Mode I fracture mechanical values of bonding pastes *for small aircraft* were determined. TLR was compared to a trial compound of a newly developed bonding paste at temperatures ranging from −40 °C to +45 °C. To the best of the authors' knowledge, the present work constitutes the first such publication. Specific fracture energies between 482 and 830 J/m^2 and notch tensile strengths between 14.8 and 22.8 MPa were measured for the bonding pastes in bulk. For the interfaces between bonding pastes and GFRP, the specific fracture energies were between 178 and 218 J/m^2 and the notch tensile strengths were between 12.1 and 15.2 MPa.
3. Knowing the properties of the new bonding paste, it was possible to modify the mixture in order to tailor its properties towards the "reference material", i.e., TLR. Three modified blends of bonding paste were tested in the bulk form at room temperature. An improvement of the specific fracture energy of up to 28% was measured.
4. The influence of adherend pre-treatment on the fracture mechanical properties of the bonding paste to GFRP interface was studied. Adherend pre-treatment, which consisted of creating a rough surface by means of peel ply, caused a small increase in both the specific fracture energy and the notch tensile strength. The improvement is smaller than the statistical uncertainty due to the low number of specimens; nevertheless, it seems logical.

Acknowledgment

The authors would like to thank Hexion Specialty Chemicals (Germany) for providing the majority of the materials used in this research.

References

[1] ASTM D5041-98(2004). Standard test method for fracture strength in cleavage of adhesives in bonded joints. West Conshohocken, PA: American Society for Testing Materials.

[2] Sener JY, Ferracin T, Caussin L, Delannay F. On the precision of the wedge-opened double cantilever beam method for measuring the debonding toughness of adhesively bonded plates. Int J Adhes Adhes 2002;22:129–37.
[3] ASTM D5045-99. Standard test methods for plane-strain fracture toughness and strain energy release rate of plastic materials. West Conshohocken, PA: American Society for Testing Materials.
[4] Liu C, Huang Y, Stout MG. Enhanced mode-II fracture toughness of an epoxy resin due to shear banding. Acta Mater 1998;46(16):5647–61.
[5] Araki W, Nemoto K, Adachi T, Yamaji A. Fracture toughness for mixed mode I/II of epoxy resin. Acta Mater 2005;53:869–75.
[6] Zhong Z, Zheng S, Huang J, Cheng X, Guo Q, Wei J. Phase behaviour and mechanical properties of epoxy resin containing phenolphtalein poly(ether ether ketone). Polymer 1998;39(5):1075–80.
[7] Girard-Reydet E, Sautereau H, Pascault JP. Use of block copolymers to control the morphologies and properties of thermoplastic/thermoset blends. Polymer 1999;40:1677–87.
[8] Ochi M, Shimaoka S. Phase structure and toughness of silicone-modified epoxy resin with added silicone graft copolymer. Polymer 1999;40:1305–12.
[9] Ochi M, Takemiya K, Kiyohara O, Nakanishi T. Effect of the addition of aramid-silicone block copolymer on the phase structure and toughness of cured epoxy resins modified with RTV silicone. Polymer 2000;41:195–201.
[10] Lowe A, Kwon OH, Mai YW. Fatigue and fracture behaviour of novel rubber modified epoxy resins. Polymer 1996;37(4):565–72.
[11] Kim HS, Khamis MA. Fracture and impact behaviours of hollow micro-sphere/epoxy resin composites. Composites Part A 2001;32:1311–7.
[12] Kitey R, Tippur HV. Role of particle size and filler-matrix adhesion on dynamic fracture of glass-filled epoxy. I. Macromeasurements. Acta Mater 2005;53:1153–65.
[13] Kawaguchi T, Pearson RA. The effect of particle-matrix adhesion on the mechanical behavior of glass filled epoxies. Part 2. A study on fracture toughness. Polymer 2003;44:4239–47.
[14] Imanaka M, Takeuchi Y, Nakamura Y, Nishimura A, Iida T. Fracture toughness of spherical silica-filled epoxy adhesives. Int J Adhes Adhes 2001;21:389–96.
[15] Xu LR, Bhamidipati V, Zhong WH, Li J, Lukehart CM, Lara-Curzio E, et al. Mechanical property characterization of a polymeric nanocomposite reinforced by graphitic nanofibers with reactive linkers. J Compos Mater 2004;38(18):1563–82.
[16] Brown EN, White SR, Sottos NR. Microcapsule induced toughening in a self-healing polymer composite. J Mater Sci 2004;39:1703–10.
[17] Kumar P, Tiwari S, Singh RK. Characterization of toughened bonded interface against fracture and impact loads. Int J Adhes Adhes 2005;25:527–33.
[18] Tschegg EK. Prüfeinrichtung zur Ermittlung von bruchmechanischen Kennwerten sowie hiefür geeignete Prüfkörper (Testing device for the determination of fracture mechanical characteristic values and appropriate test specimens). Austrian Patent Specification No. 390328, 1986 [in German].
[19] Tschegg EK. New equipments for fracture tests on concrete. Materialprüfung (Mater Test) 1991;33:338–42.
[20] Bažant Z, Planas J. Fracture and size effect in concrete and other quasibrittle materials. Boca Raton, FL: CRC Press LLC; 1998.
[21] Kettunen PO. Wood, structure and properties. Uetikon-Zürich: Trans Tech Publications Ltd.; 2006.